International Journal of Multiphase Flow 165 (2023) 104483

Contents lists available at ScienceDirect

International Journal of Multiphase Flow

journal homepage: www.elsevier.com/locate/ijmulflow

Effect of the down-slope on the structure and the pressure loss of an oil-water stream

Riccardo Attilio Franchi, Igor Matteo Carraretto *, Gregorio Chiarenza, Giorgio Sotgia, Luigi Pietro Maria Colombo

Dipartimento di Energia, Politecnico di Milano, Via Lambruschini 4, Milano 20156, Italy

ARTICLE INFO

Keywords:
Core-annular flow
Heavy oil
Inclined flow
Pressure drop
Holdup

ABSTRACT

The methodology and the results of an experimental campaign aimed at characterizing a two-phase flow of an oil-water-mixture in downward inclined pipes are here described. The goal was to assess the effects of the downslope on an oil-water stream in terms of flow patterns, pressure gradients and phase holdup inside a 40 mm I.D. pipe. The experiments ranged within $(0.56 - 1.06\ \frac{m}{s})$ and $(0.66 - 1.33\ \frac{m}{s})$ oil and water superficial velocities, respectively. The transition from annular to stratified-wavy flow pattern was analyzed and showed to occur at lower oil velocities with respect to the horizontal configuration. The frictional pressure gradients were measured, the results compared to mechanistic and empirical models showed to be in good agreement. The phase holdups were measured by quick-closing valves and compared to horizontal configuration results and literature models. Eventually, the drift-flux model was implemented confirming its applicability and a relationship for the of oil holdup was derived.

1. Introduction

A huge amount of unexploited unconventional hydrocarbon resources is represented by heavy oil, which is crude oil that has a viscosity higher than 20 *cP* and an API gravity lower than 22.3°. The incorporation of such resources into the energy market will be needed to replace the declining production of conventional light and middle oil reservoirs (Martínez-Palou et al., 2011; Saniere et al., 2004). However, among the many oil-water two-phase phenomena involved in the petroleum industry, the main technological issue for the exploitation of such crude oils regards the transportation by means of pipelines (Bannwart, 2001). In fact, huge pumping power and costly additional actions to ensure the flow are required to continuously transport crude oil through pipelines. A promising tool to handle the problem is the lubricated piping, in which oil-water core-annular (CAF) flow regime is established. Since water surrounds the oil core and wets the internal pipe walls, the longitudinal pressure drop in the pipeline is reduced down to one comparable to the flow of water alone in the pipe at the mixture total flow rate. On the other hand, this pressure reduction capability is lost when the transition to stratified-wavy flow occurs, resulting in a sudden increase in the pressure drop (Sotgia et al., 2008).

In this context, the widespread occurrence of multiphase flow in industrial applications and the specific transportation problem of heavy oils has motivated extensive research in the field. However, most of the previous studies on oil-water core-annular flow have been performed in horizontal and vertical pipe configurations, whereas not much is known about the characteristics of oil-water flow in either upward or downward inclined conditions. Therefore, the present work aims at filling the gap characterizing the oil-water core-annular flow in a downward inclined pipe.

In more detail, the objectives of the work are:

- The development of a suitable experimental facility and procedure to perform pressure drop and phase holdup measurements;
- The experimental determination of the flow patterns, pressure gradients and phase holdup during two-phase flow of very viscous oil-water mixture in downward inclined pipe configuration;
- The assessment of the locus of the critical transition from annular to wavy-stratified flow;
- The comparison of the experimental results of phase holdup and distributed pressure drop with existing empirical and mechanistic models found in the open literature.

2. Literature review

A summary of the past experimental works present in the open literature on oil-water flow is provided in Table 1, while the models

* Corresponding author.
E-mail address: igormatteo.carraretto@polimi.it (I.M. Carraretto).

https://doi.org/10.1016/j.ijmultiphaseflow.2023.104483
Received 4 December 2022; Received in revised form 23 March 2023; Accepted 11 April 2023
Available online 16 April 2023

Nomenclature

$\tilde{P}_a$	Dimensionless water pressure (–)
B	Buoyancy term (–)
C_0	Distribution parameter (–)
D	Diameter (m)
f_D	Darcy friction factor (–)
g	Gravitational acceleration (m/s^2)
H	Phase holdup (–)
J	Superficial velocity (m/s)
L	Length (m)
m	Viscosity ratio (–)
p	Pressure (Pa)
q	Flow rate ratio (–)
R	Pressure drop reduction factor (–)
Re	Reynolds number (–)
U	Actual phase velocity (m/s)
V	Volume (m^3)
Y	Gravitational component (–)
z	Pipe axis coordinate (m)

Greek

β	Inclination angle (–)
χ^2	Lockhart-Martinelli parameter(–)
μ	Dynamic viscosity (Pa s)
Ω	Cross sectional area (m^2)
ρ	Density (kg/m^3)
ϵ	Volume input fraction (–)

Subscripts

a	Annulus
c	Core
D	Darcy
f	Frictional
m	Measured
mix	Mixture
o	Oil
s	Pipe wall
w	Water

evaluated in this work are reported in Table 2. It is seen that very few experimental research is published regarding oil-water inclined flow.

Sotgia et al. (2008) experimentally analyzed oil-water core-annular flow in horizontal pipes, providing flow patterns maps, pressure drop measurements and an empirical criterion to identify the transition boundary from annular to wavy-stratified flow pattern. Grassi et al. (2008) presented the flow pattern map and pressure drop analysis for high viscosity oil-water flow through horizontal and slightly inclined pipes. No particular deviations related to the inclination angle were found in terms of flow patterns and pressure gradients. They used the two-fluid model to predict pressure drop in the case of annular flow but did not draw any conclusion regarding the transition boundary to stratified flows. Rodriguez et al. (2009) studied horizontal and vertical oil-water core-annular flows. They measured the pressure drop for different pipe diameters and materials. They suggested a more refined model to predict frictional pressure gradient, starting from the one proposed by Prada and Bannwart (2001). The results of an field-scale experiments with a steel pipe were also discussed. Strazza et al. (2011) provided an experimental analysis of very viscous oil-water flow in horizontal and slightly inclined systems in terms of pressure gradients, flow maps and phase holdup. They compared the experimental results of pressure gradients and phase holdups to the predictions of the main mechanistic and empirical models from the open literature. Ghosh et al. (2011) conducted experiments on the downflow of oil-water mixtures in vertical glass pipes. The pressure drop and flow patterns were analyzed and the Two-Fluid model was used to predict the frictional pressure gradient. An empirical correlation was also proposed to improve predictions. Colombo et al. (2012) studied the transition from annular to wavy-stratified oil-water flow within horizontal and slightly upward inclined pipes. Flow pattern visualization were taken in order to develop flow pattern maps. The transition boundary between annular and wavy-stratified flow pattern was analytically determined and overlapped to flow pattern maps showing a good agreement.

Regarding predictive models, the following were taken from the literature, representing respectively a fully empirical approach and a mechanistic design.

2.1. Arney et al. (1993)

Arney et al. (1993) measured the pressure drop and holdup of viscous oil-water mixture on an horizontal pipe with different input flow rates. An empirical correlation for water holdup H_w in terms of input water fraction ϵ_w that fits a large set of experimental data was thus proposed by the authors:

$$H_w = \epsilon_w[1 + 0.35(1 - \epsilon_w)]. \tag{1}$$

This empirical formulation has been validated by many other researchers on new experimental results, providing good estimations.

Given a reliable estimate for the holdup, the authors developed a model for the prediction of pressure gradient of oil-water vertical core-annular flow. An analogy to the Reynolds number was provided by applying the Navier-Stokes equation to the perfect liquid-liquid laminar core annular flow (PCAF) for both upward and downward core flows.

$$Re^* = \left(\frac{\rho_{mix} DJ}{\mu_w}\right)[1 + \eta^4(m - 1)] \tag{2}$$

$$\eta = \frac{D_o}{D} = \sqrt{1 - H_w} \tag{3}$$

$$m = \frac{\mu_w}{\mu_o} \tag{4}$$

$$\rho_{mix} = \rho_w H_w + \rho_o(1 - H_w) \tag{5}$$

where ρ_{mix} is the mixture actual density, J is the mixture superficial velocity and D_o is the oil core diameter. The Darcy friction factor f_D is expressed, in case of laminar-laminar CAF, by:

$$f_D = \frac{64}{Re^*} - B. \tag{6}$$

While for laminar-turbulent flow with the Blasius formulation:

$$f_D = \frac{0.316}{Re^{*0.25}} - B \tag{7}$$

where B is the additive buoyancy term that is introduced for inclined flows. The inclination angle β is considered through $\sin\beta$, to get the component of gravitational force parallel to the flow.

$$B = \frac{2\Delta\rho g \sin\beta D(1 - \eta^2)\eta^2[1 + \eta^2(m - 1)]}{\rho_o J^2[1 + \eta^4(m - 1)]} \tag{8}$$

Then, knowing the friction factor, the frictional pressure gradient in CAF is estimated following the Darcy-Weisbach equation.

Subsequently, Shi et al. (2017) updated the Arney's model adding a correction factor that accounts for the oil phase eccentricity inside the continuous water annulus. The water holdup modifies as:

$$H_w = \epsilon_w[1 + 0.31(1 - \epsilon_w)]E, \tag{9}$$

where E is the correction factor that accounts for the oil core eccentricity:

$$E = \exp\left[-0.31\left(\frac{1}{Fr}\right)^{1.067}(1 - \epsilon_w)^{0.67}\right], \tag{10}$$

Table 1
Literature experimental works on oil-water flow. Dynamic viscosities considered at 20 °C.

Author	Orientation	Diameter [mm]	μ_o [Pa s]	ρ_o [kg/m^3]
Sotgia et al. (2008)	Horizontal	21–40	0.92	889
Grassi et al. (2008)	Horizontal and ±15°	21	0.80	886
Rodriguez et al. (2009)	Horizontal and vertical	27–75	0.50	925
Strazza et al. (2011)	−10° to +15°	21	0.90	886
Ghosh et al. (2011)	Vertical	12	0.2@27 °C	960
Colombo et al. (2012)	Horizontal and +6°	21.5–50	0.9	890

Table 2
Models from the open literature.

Author	Phase holdup	Pressure gradient
Arney et al. (1993)	Empirical correlation	Empirical model
Ullmann and Brauner (2004)	Mechanistic Two-Fluid	Mechanistic Two-Fluid

and Fr is the Froude number, which represents the ratio between inertia to buoyancy forces:

$$Fr = \frac{J_o}{\sqrt{gD\frac{\rho_w-\rho_o}{\rho_o}}}, \tag{11}$$

The factor E approaches the value 1 when the core is almost concentric and has a value included between 0 and 1 when the eccentricity is more pronounced. In this work g has been replaced with $g\cos\beta$ to take into account the pipe inclination.

2.2. Ullmann and Brauner (2004)

Brauner (1991) (Bannwart, 2001) developed a mechanistic model for horizontal and inclined oil-water concentric core-annular flow using the Two-Fluid Model. Ullmann and Brauner (2004) then provided new closure relations for the wall τ_s and the interfacial τ_i shear stresses. The new closure relationships represent the effect of the inclination and the interaction between the flows of the two phases. With the new closure relations, the two-fluid model yields the exact solution for the holdup and pressure drop in case of laminar horizontal or inclined CAF. The same structures of closure relations are applied also in turbulent flows but the solution is not explicit and requires a trial and error procedure.

Assuming fully developed flow, the integral form of the momentum equations for the core (o) and annulus (w) regions are:

$$\begin{cases} -\frac{dP}{dz}\Omega_o \mp \tau_i S_i + \rho_o g \sin\beta\Omega_o = 0 \\ -\frac{dP}{dz}\Omega_w \pm \tau_i S_i - \tau_s S + \rho_w g \sin\beta\Omega_w = 0 \end{cases} \tag{12}$$

Being the two pressure gradients equal, the two equations reported in Eq. (12) modify as:

$$\tau_s \frac{S}{A_w} - \tau_i S_i \left(\frac{1}{A_w} + \frac{1}{A_o}\right) - g\sin\beta\left(\rho_w - \rho_o\right) = 0. \tag{13}$$

Where τ_i is the interfacial shear stress, which is the shear stress exerted by the annular phase on the oil core, and τ_s, the pipe wall shear stress. The structure of the closure relations for the wall and interfacial shear stresses to be used in the combined momentum equation is the following:

$$\tau_i = -\frac{1}{2}\rho_o f_i U_o (U_o - c_i U_w); \tag{14}$$

$$\tau_s = -\frac{1}{2}\rho_w f_w U_w (U_w(1 + Y F_w)) \tag{15}$$

where,

$$f_i = C_o Re_o^{-n_o} F_i;\ c_i = c_i^0 + Y F_{ci};\ Y = \frac{\Delta\rho g \sin\beta}{\left(-dp/dz_f\right)_{ws}} \tag{16}$$

$$F_{ci} = 4H_w(1 - H_w)\left[1 + \frac{2 - H_w}{2H_w}\ln(1 - H_w)\right] \tag{17}$$

and

$$f_w = C_w Re_{ws}^{-n_w}; \tag{18}$$

$$F_w = H_w(1 - H_w)\left[2 - H_w + \frac{2(1 - H_w)}{H_w}\ln(1 - H_w)\right] \tag{19}$$

The factor F_i is to account for possible augmentation of the interfacial shear due to interfacial waviness or other irregularities, it can be put $F_i = 1$ since the model in CAF is less sensitive to the estimation of the interfacial friction factor (Ullmann and Brauner, 2004). The coefficients for laminar flow of the oil core are $C_o = 16$, $n_o = 1$, while for turbulent flow of water annulus are $C_w = 0.046$, $n_w = 0.2$, $c_i^0 = 1.15 \div 1.20$ (for this study a value of c_i^0 equal to 1.16 was used) and $c_i = 1.05 \div 1.12$.

Using the above closure relations (14) and (15), the general dimensionless form of the combined momentum equation reads:

$$F_i \tilde{R}_o^{\,n_o-5}\left[1 - \tilde{R}_o^{\,2}(1 + \frac{c_i}{q})\right](1-\tilde{R}_o^{\,2}) - (1+YF_w)\chi^2 + Y\chi^2(1-\tilde{R}_o^{\,2})^3 = 0 \tag{20}$$

Which is an implicit equation in $\tilde{R}_o = R_o/R$ dimensionless core radius, which is related to the oil holdup $H_o = \tilde{R}_o^{\,2}$. The Lockhart-Martinelli parameter χ^2, taken as the ratio of the oil alone to the water alone pressure gradient (alone means that the phase flows with the superficial velocity), is used to correlate pressure gradients and holdup data.

Explicit analytical solution of Eq. (20) for $\tilde{R}_o$ can be obtained in the case of any inclination angle, but laminar core and annulus (Lc-La). Explicit solution are obtained as well in the case of $Y = 0$ (horizontal flow, or $\Delta\rho = 0$) with laminar core and turbulent annulus (Lc-Ta). However, for inclined downflow with laminar core and turbulent annulus the equation is implicit and iterative procedure is needed to get solution.

The frictional pressure gradient is expressed in terms of dimensionless parameters as:

$$\Gamma_f = \frac{-\left(\frac{dp}{dz}\right)_f}{-\left(\frac{dp}{dz}\right)_{f,ws}} = -(\tilde{P}_a + H_o Y);\ \tilde{P}_a = \frac{dp/dz - \rho_w g\sin\beta}{\left(-dp/dz_f\right)_{ws}}. \tag{21}$$

Where $\tilde{P}_a$ is a dimensionless parameter representing the contribution of water to the pressure gradient, which is function of the oil holdup by the dimensionless oil core radius $\tilde{R}_o$; Y is the dimensionless gravitational component, hence the parameter that contains the information about the inclination angle effect. The frictional pressure gradient of water in single-phase flow is computed as:

$$\left(-\frac{dp}{dz_f}\right)_{ws} = \frac{\rho_w}{2D} J_w^2 f_D \tag{22}$$

$$f_D = 0.316 Re_{ws}^{-0.25} \tag{23}$$

Sun et al. (2022) revised the approach presented above to take into account the core eccentricity and its non-circular shape by a three-zone model using an empirical correlation for the water-annulus thickness on top of the pipe. Prediction errors decreased slightly compared to the models that do not consider the above-mentioned effects, with a relative error of ±10%. However, the improvement with respect to the Arney's model lies within the experimental uncertainty of the data presented in this paper, i.e., from 2% to 8%, thus the model was not implemented.

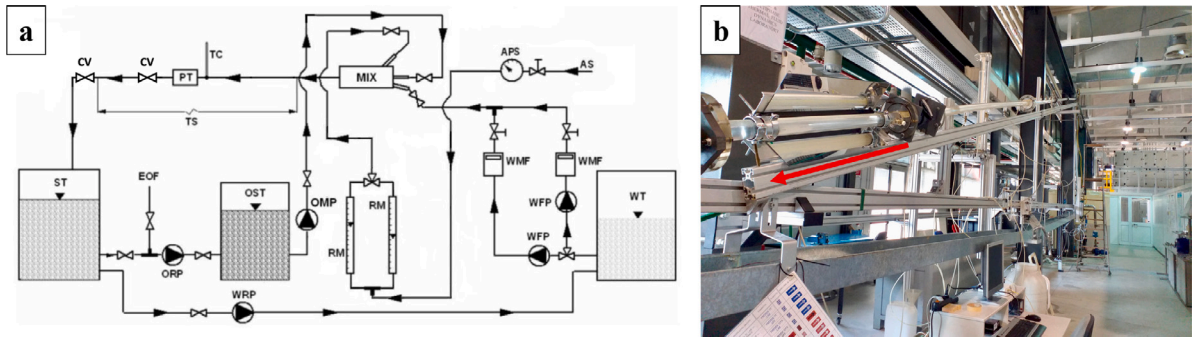

Fig. 1. (a) Experimental facility layout: (WT) water tank, (ST) separation tank, (OST) oil tank, (TS) test section, (CV) closing valves, (MIX) multiphase injector, (WFP) feedwater pump, (OMP) oil pump; (b) Plant view.

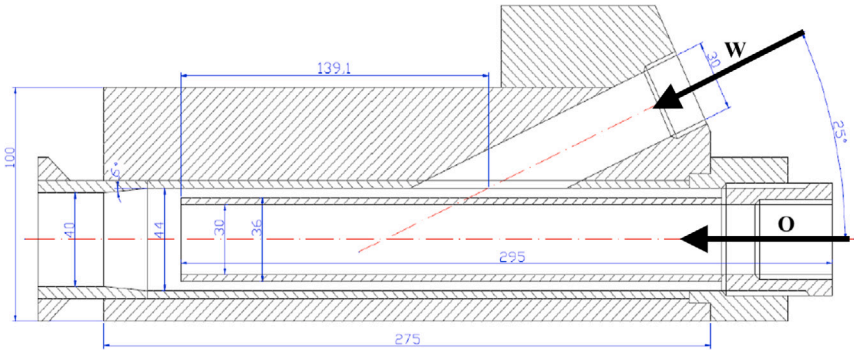

Fig. 2. Oil-water injector technical drawing. Lengths in mm and angles in degrees.

Table 3
Rheological properties of test fluids.

Fluid	ρ [kg/m^3]	μ [Pa s]
Water	999	0.001
Oil emulsion	890	0.838 (@24.5 °C)

Table 4
Oil and water superficial velocities.

J_o [$\frac{m}{s}$]	J_w [$\frac{m}{s}$]
0.56	0.66
0.71	0.88
0.91	1.10
1.06	1.33

3. Experimental setup

3.1. Description of the test facility

The oil-water flow test loop is described in Fig. 1. The pipeline, 20 m long and 40 mm I.D., was downward inclined of 15° with respect to the horizontal, which leads to the maximum height achievable in the laboratory. All the angles tested in the literature are smaller, except for Strazza et al. (2011), in which case, however, the pipe diameter is about half. The test fluids used in the current study are tap water from the municipal network and a stable emulsion of water and Milpar 220 mineral oil. The rheological properties of the two fluids are reported in Table 3. In particular, the oil viscosity is assumed constant at the average test temperature of the fluids (day-by-day fluctuations did not exceed 0.5 °C). The measured oil-water interfacial tension is 0.020 N/m (Sotgia et al., 2008).

Oil and water are pumped into the Plexiglas® pipe from their storage tanks, the water flow rate is controlled by a valve and measured by means of a magnetic flowmeter while the flow rate of oil is set by regulating the speed of a gear pump by an inverter through a calibration curve. The fluids are introduced into the pipe by a suitably designed injector promoting the development of the core-annular flow pattern (Fig. 2). The fluids are collected at the end of the test section in a separation tank, where they naturally separate in about 30 to 45 min and then are recirculated to the respective storage tanks.

The pressure drop and phase holdup measurements are performed at 6 m (150 diameters) from the injector to enable flow development, according to the considerations reported in Grassi et al. (2008). The pressure drop measurements are taken by a differential piezo-resistive pressure transducer C230 Setra System (Range 0–7 V, Output 0.5–5.05 kPa, Accuracy ± 0.5% of the full scale) on a 2 m test section equipped with 5 static pressure taps. Phase holdup measurements are performed at the end of the test section by *quick-closing* valves, as reported in Colombo et al. (2015). Moreover, two mirrors at 90° are arranged in order to take pictures with three views: central, upper and lower. The data are collected via a data acquisition board and processed by means of LabView® and Excel®.

3.2. Experimental procedure

Four different oil superficial velocities and four water superficial velocities were selected (see Table 4), having a total of 16 couples of operating conditions.

Photographic analysis, pressure drop and phase holdup experiments were carried out as per the procedures reported.

3.2.1. General procedure

1. Once the oil and water are separated by gravity in the dedicated tank (ST) (~30 min) the water is firstly recovered by a centrifugal pump in the water tank (WT) and then the oil is pumped with a recirculating gear pump to the oil tank (OST).

2. The water that remains at the bottom of the oil tank is removed with a pump towards the separation tank.
3. The quick-closing valves are opened.
4. Water pump is turned on and the pipe is flushed for 2 min, then a high flow rate is set until no air is present within the pipe. Then the desired flow rate is set plus a 0.3 $\frac{m^3}{h}$ to compensate for the reduction once oil enters in the pipe.
5. The desired flow rate of oil is set from the inverter panel and the pump is turned on. A two-phase flow sets into the pipe. The water flow rate is adjusted to the desired one, the flow is let developing. Once developed the facility is ready for the tests.
6. After performing the tests, the oil pump is firstly switched off, immediately the water flow rate is increased and the oil valve is closed. This allows to avoid oil sticking to the pipe walls.
7. Quick closing valves are closed leaving the pipes full of water, this helps reducing the charging time.

3.2.2. Photographic campaign

The pictures were taken with a NIKON D4 camera with a NIKKOR 60 mm f/2.8G Micro lens, setting an exposure time of 1/6400 s with a F-stop of f/16.

1. The oil flow rate is set and kept fixed throughout the run.
2. Water flow rate is set and multiphase flow is left to fully develop and stabilize.
3. Pictures are taken, framing in the photo a reference to the oil and water flow rates.
4. Water flow rate is changed, with fixed oil flow rate, leaving 30 s for the flow to develop. The same procedure is repeated for all the water flow rates.

3.2.3. Pressure drop experiments

The experimental runs were repeated 10 times for each condition and then the arithmetic mean as well as the standard deviation were registered for all the measured quantities. The uncertainty on the measured quantities resulted always lower than 10%, ranging from a minimum of 2% to a maximum of 8%.

1. During the preliminary flow of only water the pressure taps are cleaned by opening the related valves and disconnecting the pressure commutator from the pressure transducer. In this way air and oil deposits are removed.
2. During the tests, which last for ~ 1 min, pressure taps are put in connection to the transducer.
3. Once the test-runs are done, the general test ending procedure is followed. Then the log generated by LabView® is copied and pasted on Excel® to check the results.
4. The pressure drop tests are checked by plotting the pressure data against the distance. The points are expected to lie on a straight line with negative slope.

3.2.4. Holdup experiments

The experimental runs were repeated 10 times for each condition and then the arithmetic mean as well as the standard deviation were registered for all the measured quantities. The uncertainty on the measured quantities is about 2%.

1. The desired flow rates combination is set and the flow is let to develop.
2. Two operators have to perform this experiment. One operator has to turn off all the pumps (using a release button), whereas the other closes the two valves (the distance between the two valves is of 1.10 m).
3. The fluids are left to naturally separate inside the test pipe for ~ 15 min.
4. After having measured the tare of a plastic beaker, the water is spilled from the pipe.
5. The beaker is weighted once more, and the net weight of the water spilled from the pipe into the beaker is retrieved and used to determine the water holdup.

4. Experimental results

4.1. Photographic analysis

A photographic analysis was conducted to qualitatively check the effects of the inclination angle on the flow patterns and the transition to stratified-wavy flow. In particular, the oil core was always present, but affected by a certain degree of eccentricity that decreased with increasing oil superficial velocity J_o and total flow rate. Pictures for each flow condition were collected in a matrix and reported in Fig. 3. Specifically, at fixed superficial oil velocity J_o we can see similarities in the flow pattern evolution, i.e., an increase in the oil dispersion as the water flow rate increases. On the other hand, also at fixed superficial water velocity J_w we can see a pattern in the flow evolution, i.e., an increase in the oil core and an eccentricity reduction as the oil flow rate increases. Eventually, as an example Fig. 4 shows two flow regimes where the oil and water flow rates are increased: the result is a reduced eccentricity. Oil drops detachment from the core to the continuous water layer became more present at high water superficial velocities ($J_w = 1.11 - 1.33$ $\frac{m}{s}$), whereas at the lowest water superficial velocities (i.e., $J_w = 0.66$ $\frac{m}{s}$) only few oil drops detached from the core.

In Fig. 5 the flow pattern map of the inclined pipe is reported. Generally, the results indicate that the flow patterns that occurred in case of inclined pipe are similar to the ones of the horizontal configuration reported in Sotgia et al. (2008), specifically all the operating conditions fall in core-annular region.

Moreover, the transition from annular to wavy-stratified flow pattern is critical since, as the oil core sticks to the pipe walls, it induces a sharp increase in the pressure gradient, which in real operating conditions might cause chugging. Hence, an analysis was performed to check how the transition was affected by inclination. The validity of the transition boundary defined by Colombo et al. (2012) for the 40 mm I.D. horizontal pipe was thus experimentally checked. At constant oil flow rate, the water flow rate was decreased until large Kelvin-Helmholtz waves were observed on the lower portion of the oil core, which is the signal that – on the top – oil has stuck to the wall. At the same time, the upper portion of the pipe gets dirty with the oil. The instability mechanism leading to the break-up of the thin top-wall film due to the floating of the oil core has been widely studied by Brauner and Maron (1992) in the case of concentric core. Furthermore, Huang and Joseph (1995) showed that eccentric flow is stable when concentric flow is stable. However, the data shown in Sotgia et al. (2008) and Colombo et al. (2012) showed only qualitative agreement with the transition boundary predicted by the stability analysis reported in Brauner and Maron (1992).

The transition suddenly occurs over the whole pipeline even very close to the injection point (about 5 diameters). However, it was not possible to determine a relationship between the mixture velocity and the distance from the injection at which the transition extends to the whole pipeline, because of the fouling of the upper portion of the pipe.

A total of six oil flow rates were considered to properly identify the transition boundary, a graphical representation of the tests is reported in Fig. 6. The critical transition appeared for oil superficial velocities ($J_o < 0.4$ $\frac{m}{s}$) lower than expected for the horizontal configuration, while for higher velocities the oil core smoothly expanded without fouling the pipe. A new approximate boundary was hence defined:

$$J_w = 0.7745 - 1.9091 J_o \tag{24}$$

Qualitatively, this result is not surprising if it is considered that oil comes in contact with the pipe wall owing to buoyancy forces. In particular, the critical transition arises when the latter overcome inertia forces. In the horizontal pipe, the acceleration due to gravity

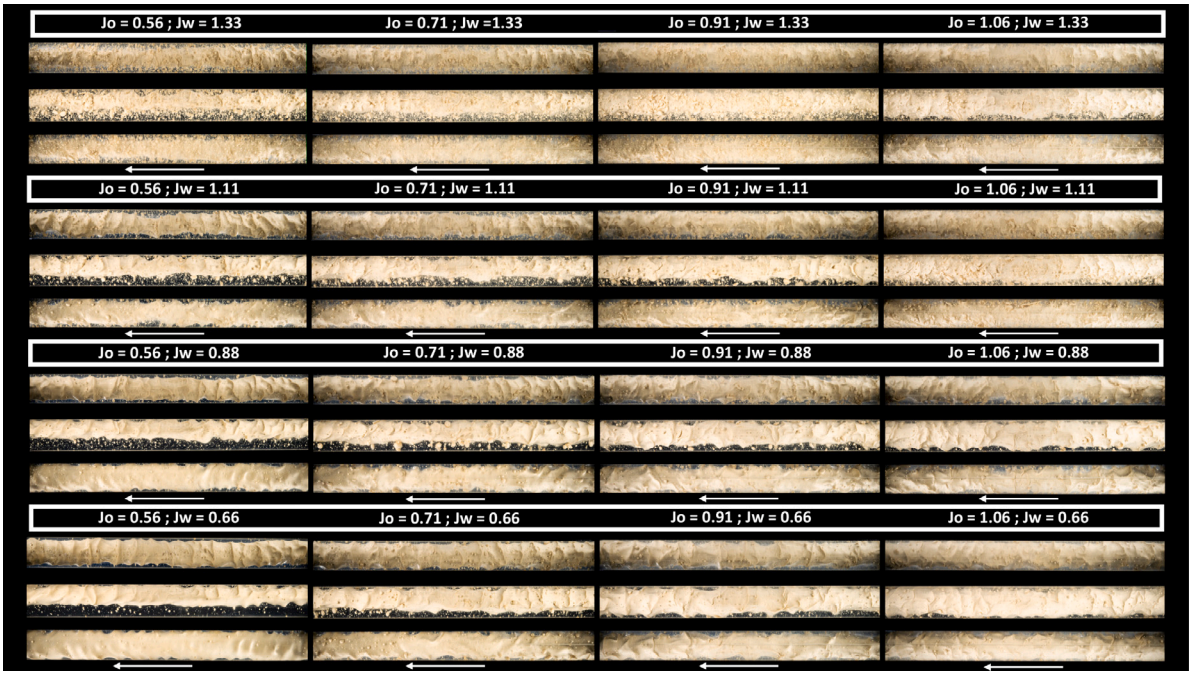

Fig. 3. Matrix of the flow regimes photos. The superficial velocities are in $\frac{\mathrm{m}}{\mathrm{s}}$, the flow direction is given by the arrow.

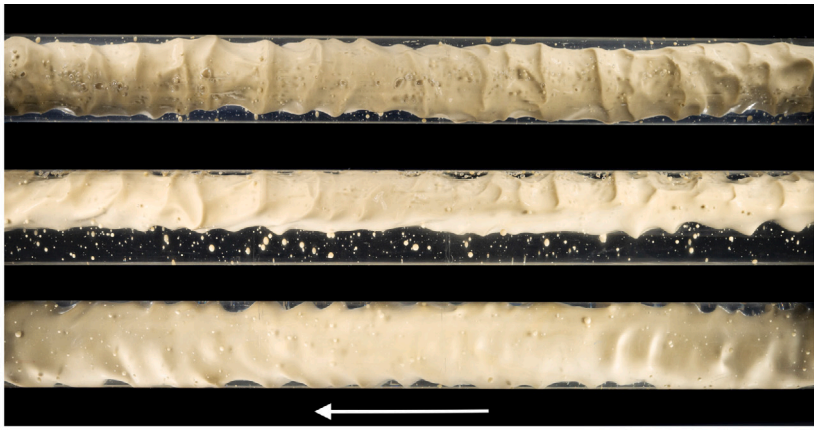

(a) $J_o = 0.56\ \frac{m}{s};\ J_w = 0.66\ \frac{m}{s}$

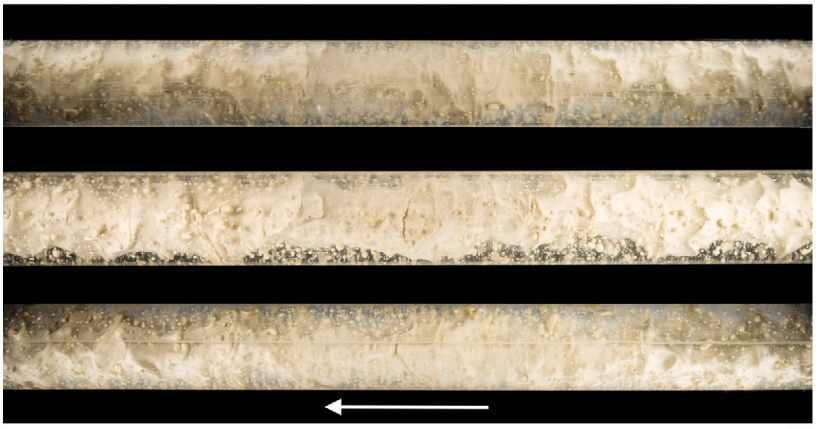

(b) $J_o = 1.06\ \frac{m}{s};\ J_w = 1.33\ \frac{m}{s}$

Fig. 4. Total flow momentum effect on the flow patterns, (a) minimum and (b) maximum total flow rate conditions. Flow direction, indicated by the arrow, is from right to left. Top, central and bottom view.

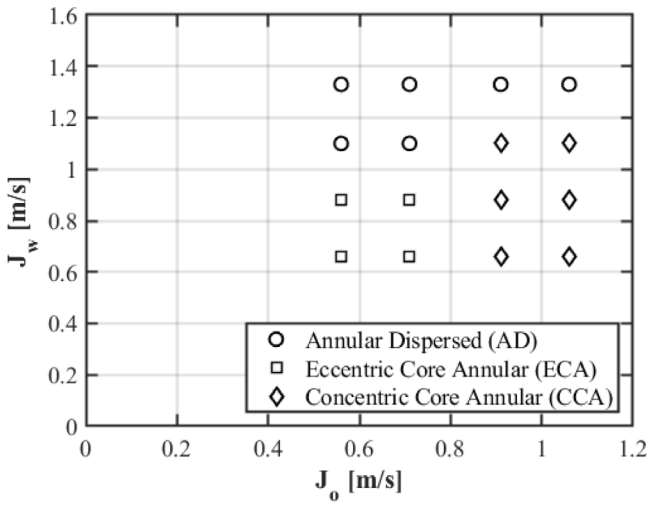

Fig. 5. Flow pattern maps for the 40 mm I.D. pipe inclined configuration $\beta = 15°$, for the horizontal configuration please refer to Sotgia et al. (2008).

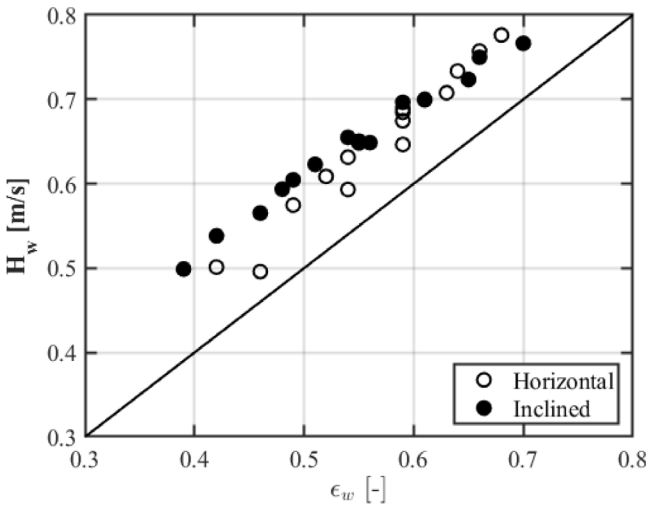

Fig. 7. Water holdup versus water input fraction. The bisector represent the homogeneous mixture condition.

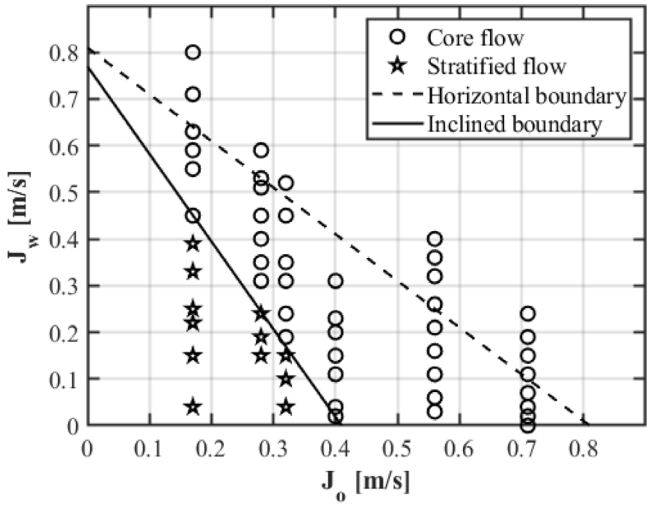

Fig. 6. Flow map of experimental runs. The dotted line represent the analytical boundary for the horizontal case; solid line is Eq. (24).

is normal to the axis (direction of principal motion), whereas in the downward inclined pipe the action of gravity can be broken up into two components: one is parallel to the axis and contributes to the momentum flow (inertia), the other is normal to the axis and, in combination with the density difference, is responsible for lifting the oil core towards the pipe wall (buoyancy). However, compared to the horizontal layout, the latter is reduced by a factor equal to $cos\ \beta$, i.e., by about 3.4%. Thus, it is expected that the transition between core-flow and stratified flow takes place at lower velocities compared with the horizontal flow.

4.2. Phase holdup

Phase holdups measured with the closing valves method described in Section 3.2 are reported in Fig. 7 in terms of water holdup H_w against the water input fraction (or water cut). It was observed that water holdup was always higher than the water input fraction, therefore the water actual velocity $U_w = \frac{J_w}{H_w}$ is always lower than the oil actual velocity $U_o = \frac{J_o}{H_o}$. This is consistent with flow visualizations showing that the oil flows in the core, though eccentric, with the water adjoining the pipe wall. In addition, by increasing water input fractions the experimental points tend to approach the bisector as the flow regime evolves to a more and more dispersed core, i.e., a pattern closer to the ideally homogeneous flow, for which the phase holdup equals the input fraction. In order to better understand the effects of the inclination on the actual velocities a comparison with horizontal configuration data in the same experimental conditions was performed. The horizontal data were available from previous works Colombo et al. (2015). The comparison showed that the oil actual velocity in the inclined configuration is higher than in the horizontal case, for the operating conditions characterized by $\epsilon_w < 0.6$. This result supports the evidence, given in the previous section, that at the same superficial velocities the flow conditions for the downward inclined pipe lie farther from the transition boundary between core and stratified flow than for the horizontal pipe, in spite of the fact that the water is the heaviest phase, and hence should be more accelerated by gravity than oil. On the other hand, it has to be noticed that the density difference between oil and water is small and water is always in contact with the wall, hence subject to friction. As previously observed, the oil in the core is lifted up by a component of the buoyancy force reduced by the cosine of the inclination angle compared with the horizontal layout. Thus, the core should be less eccentric and possibly flow faster.

Data fitting was obtained by means of the *drift-flux* void fraction model earlier introduced by Zuber and Findlay (1965) for gas-liquid flows. Being the oil the phase traveling faster, it was replaced to the gas phase in the original model, so that:

$$U_o = C_o J + U_{o,J} \tag{25}$$

$$H_o = \frac{\epsilon_o}{C_0 + \frac{U_{o,J}}{J}} \tag{26}$$

where C_0 is the $distribution\ parameter$ that accounts for non-uniform phase distribution in the pipe cross section, J is the mixture velocity and $U_{o,J}$ is the $weighted\ mean\ drift\ velocity$, which accounts for the local relative velocity of the phases (Fig. 8).

The oil actual velocity, calculated from the measured oil holdup, is plotted against the mixture superficial velocity: it is clearly seen that the data point fall on a straight line with excellent approximation. A linear regression is thus performed to determine the slope, representing the distribution parameter, i.e. $C_0 = 1.29$, and the intercept, representing the drift velocity, i.e. $U_{o,J}$ about zero, the regression coefficient of determination (R^2) is equal to 0.98. Compared with the horizontal flow, the distribution parameter is 5.8% lower, which is consistent with the increased velocity of the oil core. As the drift-flux velocity

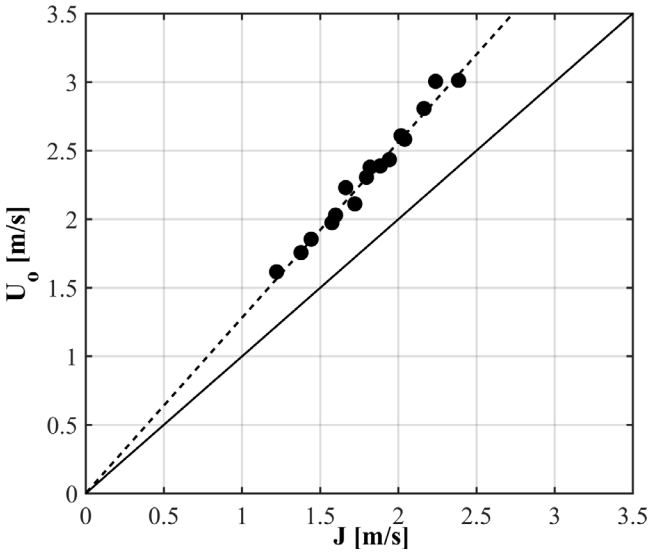

Fig. 8. Oil actual velocity against the mixture superficial velocity.

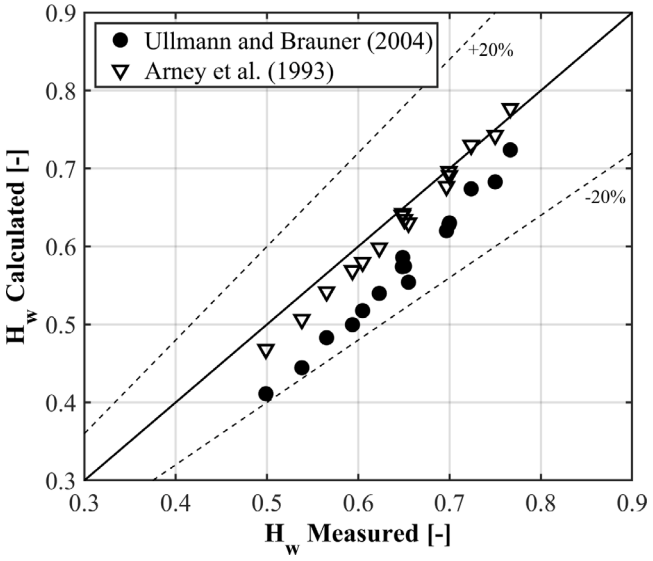

Fig. 9. Parity plot, calculated water holdup against the measured.

is practically zero (Fig. 8) the model can be simplified to $H_o = K\epsilon_o$, with $K = C_0^{-1} = 0.775$.

Eventually, the predictions of phase holdup by literature models were compared to the experimental results. The models considered were the mechanistic model of Ullmann and Brauner (2004) that needs an iterative procedure to converge to a solution, and the empirical correlations of Arney et al. and Shi et al. The results are reported in tabular form in Table 5 and in a parity plot against the measured holdup data in Fig. 9, where MRD and MARD are defined as follow (where z is a generic quantity):

$$MRD = \frac{1}{N}\sum_{i=1}^{N}\frac{z_{i,calculated} - z_{i,measured}}{z_{i,measured}}, \tag{27}$$

$$MARD = \frac{1}{N}\sum_{i=1}^{N}\frac{|z_{i,calculated} - z_{i,measured}|}{z_{i,measured}}. \tag{28}$$

The Ullmann and Brauner model tends to underpredict the water holdup, while Arney only slightly. On the other hand, the model by Shi, that takes into account the core eccentricity, does not improve the predicting performances. Anyway, all models improve their predictions as the water holdup increases. The estimate lies within the ±20% relative error range. In summary, the Arney correlation, though developed on a dataset mainly based on horizontal flows, provides better estimates (MARD = 2.79%) compared to the mechanistic one (MARD = 12.11%).

By comparison, the data fitting through the drift-flux model is reported in Table 5, obviously showing the best agreement with the data.

Table 5
Models phase holdup prediction performances.

Model	MRD [%]	MARD [%]
Ullmann and Brauner	−12.11	12.11
Drift-Flux	0.53	1.22
Arney et al.	−2.51	2.79
Shi et al.	−8.33	8.33

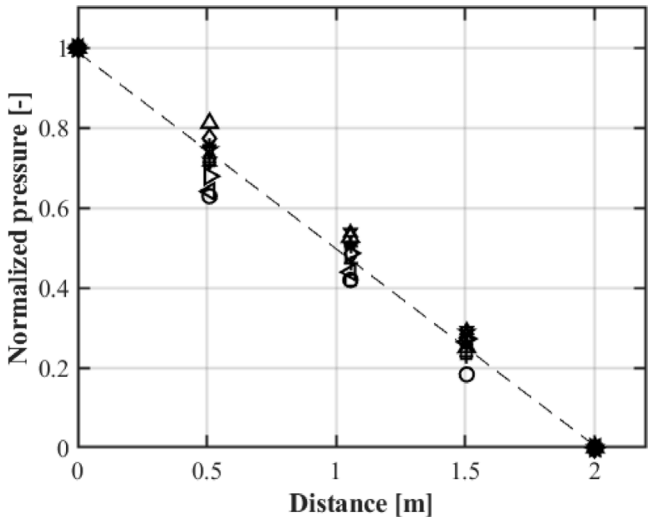

Fig. 10. Pressure drop against distance, data are normalized on the highest value and a linear regression is performed ($J_o = 0.56$ $\frac{m}{s}$ and $J_w = 0.66$ $\frac{m}{s}$).

4.3. Pressure drop

As shown from the momentum balance, the pressure gradient is the sum of three components: accelerative, gravitational and frictional. In the present case, the accelerative pressure gradient is null since the phases are incompressible and, under fully developed conditions, phase fractions are constant across the flow. The total pressure gradient was obtained from the pressure measurements taken along the flow, showing a linear decreasing behavior, which indicated that fully developed conditions have been achieved indeed, being the pressure gradient independent of the axial coordinate. As an example, Fig. 10 shows on the same plot repeated tests for a sample operating condition. Normalization has been applied to eliminate the offset caused, e.g., by the small changes in the absolute pressure between consecutive runs, such that the normalized pressure at each tap is $p_{norm} = (p - p_{min})/(p_{max} - p_{min})$. Accordingly, the first tap, i.e., the closest to the test section inlet, always has $p_{norm} = 1$, whereas the last tap always has $p_{norm} = 0$. To summarize the results, Table 6 reports the values of the average pressure gradients, their standard deviations and the coefficients of determination of the linear regression for all the tested conditions.

The frictional pressure gradient was calculated by subtraction of the gravitational component, as follows:

$$\left(\frac{dp}{dz}\right)_f = \left(\frac{dp}{dz}\right)_m + (\rho_w - \rho_{mix})g\sin\beta \tag{29}$$

where ρ_{mix} is the mixture actual density (Eq. (5)). The frictional pressure gradients are shown in Fig. 11 with their standard deviation

Table 6
Experimentally determined pressure gradients.

J_o [$\frac{m}{s}$]	J_w [$\frac{m}{s}$]	$-\frac{dp}{dz}$ [$\frac{kPa}{m}$]	SD [$\frac{kPa}{m}$]	R^2 [–]
0.56	0.66	0.468	0.023	0.999
	0.88	0.623	0.031	0.998
	1.10	0.770	0.069	0.999
	1.33	0.872	0.047	0.999
0.71	0.66	0.632	0.020	0.999
	0.88	0.774	0.051	0.999
	1.10	0.863	0.059	0.999
	1.33	1.076	0.035	0.999
0.91	0.66	0.785	0.025	0.999
	0.88	0.950	0.020	0.999
	1.10	1.066	0.046	0.999
	1.33	1.251	0.053	0.999
1.06	0.66	0.949	0.060	0.999
	0.88	1.050	0.066	0.999
	1.10	1.262	0.107	0.999
	1.33	1.346	0.061	0.999

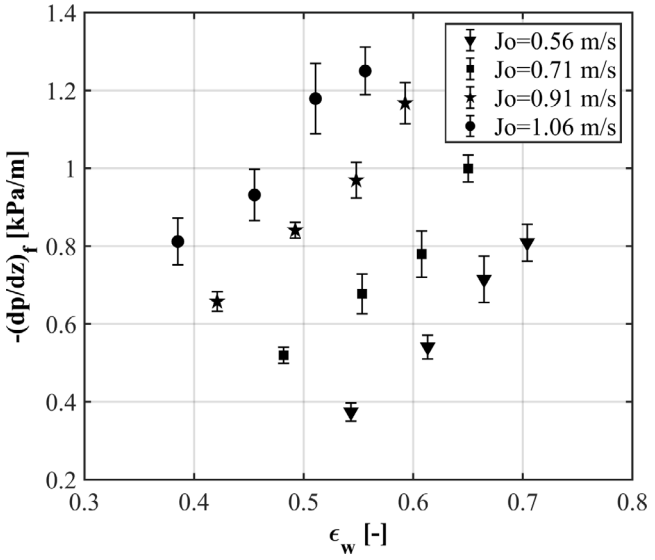

Fig. 11. Frictional pressure gradient versus the water volume input fraction.

plotted against the water input fraction ϵ_w. For each oil velocity the water superficial velocity increases from left to right as ϵ_w increases. The repeatability of the pressure drop tests was characterized by a relative standard deviation ranging between 2.41% and 8.36%.

In order to have a better visualization of the advantage introduced by CAF for the pressure drop reduction in very viscous oil transportation, the experimental pressure gradient data are reported in terms of the Pressure Drop Reduction Factor R (Sotgia et al., 2008), defined as:

$$R = \frac{\Delta p_o}{\Delta p_{wo}} \tag{30}$$

The numerator Δp_o is the pressure drop of the oil flowing alone at its flow rate, the term is calculated with the Hagen-Poiseuille law as the oil-alone flow is always laminar:

$$\Delta p_o = \frac{128 \mu_o Q_o L}{\pi D^4} \tag{31}$$

The denominator Δp_{wo} is the measured frictional pressure drop of the two-phase flow.

Accordingly, the results are reported in Fig. 12, from which it is evident that the pressure reduction capability increases with decreasing water fraction.

On the other hand, the transportation of viscous oil in core-annular flow has to be performed at the lowest possible water flow rate, but

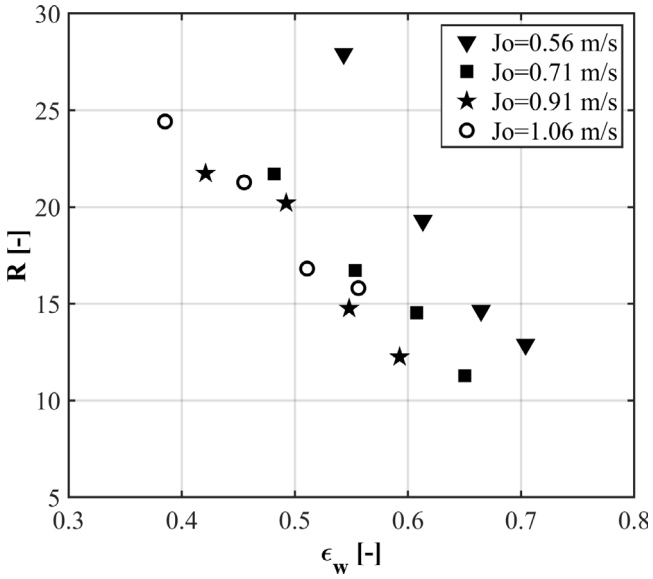

Fig. 12. Pressure drop reduction factor in function of the water input fraction.

Table 7
Models pressure drop prediction performances.

Model	MRD [%]	MARD [%]
Ullmann and Brauner	8.14	8.20
Arney et al.	−2.83	5.70

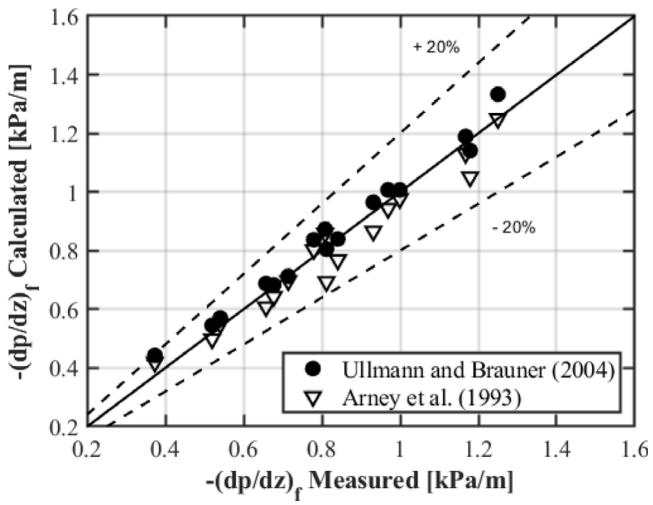

Fig. 13. Parity plot, calculated versus measured frictional pressure gradients.

sufficiently far from the conditions for the onset of the transition to stratified-wavy, which will cause issues to the mixture transportation as already anticipated. Lastly, two models available in the open literature were compared to the collected data. The mechanistic model of Ullmann and Brauner (2004), based on the Two-Fluid model for inclined configurations, and the empirical model by Arney et al. (1993). The prediction performance was evaluated in terms of Mean Relative Deviation (MRD) and Mean Absolute Relative Deviation (MARD), the results are reported in Table 7 and in a parity plot against the measured data in Fig. 13.

The model by Arney tends to slightly underestimate the pressure drop but the overall prediction shows the lowest deviation with MARD = 5.70%. Ullmann and Brauner's model tends instead to overestimate

the values, and the predictions of both models fall within the 20% relative error deviation.

Moreover, also in case of horizontal pipe configuration, the two models have a MARD that falls within the ± 20% region as already reported in Colombo et al. (2017).

5. Conclusions

The investigated flow conditions were experimentally characterized in terms of flow pattern, frictional pressure gradient and phase holdup. The dataset covered the domain of core-flows delimited by the onset of stratified flow (lower limit) and dispersed-core (upper limit). The influence of the downward inclination ($\beta = 15°$) was described in comparison with the horizontal layout ($\beta = 0°$).

It resulted that the annular/wavy-stratified transition occurred at much lower oil and water superficial velocities compared to the horizontal case at the same experimental conditions. The downslope enhances the stability of the oil-water core-annular flow possibly because the effective component of the buoyancy force on the oil core is lower and the oil actual velocity results higher. However, the data for different inclinations are still too scarce to attempt a quantitative correlation between the critical velocities and the inclination angle, which represents a further development of this work.

The phase holdups were measured by the *quick-closing* valves method and compared to horizontal pipe configurations and literature models predictions. The water holdup resulted always higher than the water input fraction, hence the oil actual velocity was always higher than the water one. In addition, the downslope increases the slip between the phases and the oil actual velocity is higher than in the horizontal case. The empirical correlation of Arney et al. provided very good agreement with the data and is thus recommended also for inclined configurations. The mechanistic model by Ullmann and Brauner (2004) led to acceptable but underestimated predictions of the water holdup. On the other hand, the Shi et al. correction to account for core eccentricity did not provide improvement in the performance predictions.

The *drift-flux* void fraction model of Zuber and Findlay, originally developed for gas-liquid systems, proved to be very effective in fitting the experimental data also for liquid-liquid flows, with MARD = 2.04%.

Eventually, the frictional pressure drop was evaluated and the results were also presented in terms of the pressure drop reduction factor, ranging between 10 and 30, which shows the benefit of the lubrication effect provided by the water annulus adjoining the wall. The frictional pressure drop is well predicted by the literature models despite the idealization of concentric core, with MARD always lower than 10%.

CRediT authorship contribution statement

Riccardo Attilio Franchi: Methodology, Software, Formal analysis, Investigation, Writing – original draft. **Igor Matteo Carraretto:** Conceptualization, Validation, Investigation, Writing – original draft, Project administration. **Gregorio Chiarenza:** Investigation, Resources, Visualization. **Giorgio Sotgia:** Conceptualization, Resources, Supervision. **Luigi Pietro Maria Colombo:** Conceptualization, Resources, Writing – review & editing, Supervision, Project administration, Funding acquisition.

Declaration of competing interest

The authors declare that they have no known competing financial interests or personal relationships that could have appeared to influence the work reported in this paper.

Data availability

Data will be made available on request

References

Arney, M., Bai, R., Guevara, E., Joseph, D., Liu, K., 1993. Friction factor and holdup studies for lubricated pipelining-I. experiments and correlations. Int. J. Multiph. Flow. 19 (6), 1061–1076. http://dx.doi.org/10.1016/0301-9322(93)90078-9, cited By 107. URL https://www.scopus.com/inward/record.uri?eid=2-s2.0-0027791150&doi=10.1016%2f0301-9322%2893%2990078-9&partnerID=40&md5=3f2d7b9a935e333c9c022c31f8baaab1.

Bannwart, A., 2001. Modeling aspects of oil-water core-annular flows. J. Pet. Sci. Eng. 32 (2–4), 127–143. http://dx.doi.org/10.1016/S0920-4105(01)00155-3, cited By 102. URL https://www.scopus.com/inward/record.uri?eid=2-s2.0-0035846492&doi=10.1016%2fS0920-4105%2801%2900155-3&partnerID=40&md5=51c3b2fc992245e89042eeb06a7e2208.

Brauner, N., Maron, D.M., 1992. Flow pattern transitions in two-phase liquid-liquid flow in horizontal tubes. Int. J. Multiph. Flow. 18 (1), 123–140.

Colombo, L., Guilizzoni, M., Sotgia, G., 2012. Characterization of the critical transition from annular to wavy-stratified flow for oil–water mixtures in horizontal pipes. Exp. Fluids 53, http://dx.doi.org/10.1007/s00348-012-1378-1.

Colombo, L.P., Guilizzoni, M., Sotgia, G., Dehkordi, P.B., Lucchini, A., 2017. Water holdup estimation from pressure drop measurements in oil-water two-phase flows by means of the two-fluid model. In: Journal of Physics: Conference Series, Vol. 923. IOP Publishing, 012012.

Colombo, L., Guilizzoni, M., Sotgia, G., Marzorati, D., 2015. Influence of sudden contractions on in situ volume fractions for oil–water flows in horizontal pipes. Int. J. Heat Fluid Flow 53, 91–97. http://dx.doi.org/10.1016/j.ijheatfluidflow.2015.03.001.

Ghosh, S., Das, G., Das, P., 2011. Pressure drop analysis for liquid-liquid downflow through vertical pipe. J. Fluids Eng. 133, 011202. http://dx.doi.org/10.1115/1.4003354.

Grassi, B., Strazza, D., Poesio, P., 2008. Experimental validation of theoretical models in two-phase high-viscosity ratio liquid-liquid flows in horizontal and slightly inclined pipes. Int. J. Multiph. Flow. 34 (10), 950–965. http://dx.doi.org/10.1016/j.ijmultiphaseflow.2008.03.006, cited By 101. URL https://www.scopus.com/inward/record.uri?eid=2-s2.0-49649117542&doi=10.1016%2fj.ijmultiphaseflow.2008.03.006&partnerID=40&md5=c49de2be1eddbdd52af665045451ac62.

Huang, A., Joseph, D.D., 1995. Stability of eccentric core–annular flow. J. Fluid Mech. 282, 233–245.

Martínez-Palou, R., de Lourdes Mosqueira, M., Zapata-Rendón, B., Mar-Juárez, E., Bernal-Huicochea, C., de la Cruz Clavel-López, J., Aburto, J., 2011. Transportation of heavy and extra-heavy crude oil by pipeline: A review. J. Pet. Sci. Eng. 75 (3), 274–282. http://dx.doi.org/10.1016/j.petrol.2010.11.020, URL https://www.sciencedirect.com/science/article/pii/S0920410510002640.

Prada, J., Bannwart, A., 2001. Modeling of vertical core-annular flows and application to heavy oil production. J. Energy Resour. Technol. Trans. ASME 123 (3), 194–199. http://dx.doi.org/10.1115/1.1377894, cited By 43. URL https://www.scopus.com/inward/record.uri?eid=2-s2.0-13544269906&doi=10.1115%2f1.1377894&partnerID=40&md5=2ff2e090e8bdc5ece7ce33b741b2bd68.

Rodriguez, O., Bannwart, A., de Carvalho, C., 2009. Pressure loss in core-annular flow: Modeling, experimental investigation and full-scale experiments. J. Pet. Sci. Eng. 65 (1–2), 67–75. http://dx.doi.org/10.1016/j.petrol.2008.12.026, cited By 51. URL https://www.scopus.com/inward/record.uri?eid=2-s2.0-60549096440&doi=10.1016%2fj.petrol.2008.12.026&partnerID=40&md5=024ef124d5a3c30821e5a04c54436786.

Saniere, A., Hénaut, I., Argillier, J., 2004. Pipeline transportation of heavy oils, a strategic, economic and technological challenge. Oil Gas Sci. Technol. 59 (5), 455–466. http://dx.doi.org/10.2516/ogst:2004031, cited By 169. URL https://www.scopus.com/inward/record.uri?eid=2-s2.0-10644282326&doi=10.2516%2fogst%3a2004031&partnerID=40&md5=cf14cec31fbae0b1b86f2900db758ff7.

Shi, J., Lao, L., Yeung, H., 2017. Water-lubricated transport of high-viscosity oil in horizontal pipes: The water holdup and pressure gradient. Int. J. Multiph. Flow. 96, 70–85. http://dx.doi.org/10.1016/j.ijmultiphaseflow.2017.07.005, cited By 10. URL https://www.scopus.com/inward/record.uri?eid=2-s2.0-85023192252&doi=10.1016%2fj.ijmultiphaseflow.2017.07.005&partnerID=40&md5=230705b180b7dab9e06485dc20e379ee.

Sotgia, G., Tartarini, P., Stalio, E., 2008. Experimental analysis of flow regimes and pressure drop reduction in oil-water mixtures. Int. J. Multiph. Flow. 34 (12), 1161–1174. http://dx.doi.org/10.1016/j.ijmultiphaseflow.2008.06.001, cited By 97. URL https://www.scopus.com/inward/record.uri?eid=2-s2.0-54449094143&doi=10.1016%2fj.ijmultiphaseflow.2008.06.001&partnerID=40&md5=a2b3eaff4c50aebb6f3e3f57eeb2169a.

Strazza, D., Grassi, B., Demori, M., Ferrari, V., Poesio, P., 2011. Core-annular flow in horizontal and slightly inclined pipes: Existence, pressure drops, and hold-up. Chem. Eng. Sci. 66 (12), 2853–2863. http://dx.doi.org/10.1016/j.ces.2011.03.053, cited By 48. URL https://www.scopus.com/inward/record.uri?eid=2-s2.0-79955016289&doi=10.1016%2fj.ces.2011.03.053&partnerID=40&md5=1501e9512a87812138834cbe65bd167f.

Sun, J., Guo, L., Fu, J., Jing, J., Yin, X., Lu, Y., Ullmann, A., Brauner, N., 2022. A new model for viscous oil-water eccentric core annular flow in horizontal pipes. Int. J. Multiph. Flow. 147, 103892.

Ullmann, A., Brauner, N., 2004. Closure relations for the shear stress in two-fluid models for core-annular flow. Multiph. Sci. Technol. 16, 355–387. http://dx.doi.org/10.1615/MultScienTechn.v16.i4.50.

Zuber, N., Findlay, J.A., 1965. Average volumetric concentration in two-phase flow systems. J. Heat Transfer 87 (4), 453–468. http://dx.doi.org/10.1115/1.3689137.